

# Local and Coupled Thermodynamic Stability of the Two-Domain and Bifunctional Enzyme SlyD from *Escherichia coli*

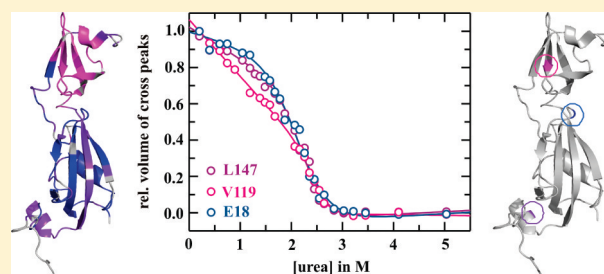
Caroline Haupt,<sup>†</sup> Ulrich Weininger,<sup>†,§</sup> Michael Kovermann,<sup>†</sup> and Jochen Balbach<sup>\*,†,‡</sup>

<sup>†</sup>Institut für Physik, Biophysik, Martin-Luther-Universität Halle-Wittenberg, D-06120 Halle (Saale), Germany

<sup>‡</sup>Mitteldeutsches Zentrum für Struktur und Dynamik der Proteine (MZP), Martin-Luther-Universität Halle-Wittenberg, D-06099 Halle (Saale), Germany

**S** Supporting Information

**ABSTRACT:** SlyD (*sensitive to lysis D*) is a protein folding helper enzyme comprising peptidylprolyl isomerase as well as chaperone activities at the respective FKBP and IF domains. Both domains coact concerning the peptidylprolyl isomerase activity on protein substrates. Using various biophysical techniques and NMR spectroscopy, the local and global thermodynamic stability of the variant (1–165) of SlyD from *Escherichia coli* (SlyD<sup>\*</sup>) was characterized. Structurally, both domains are rather independent. The urea-induced unfolding transitions of the two domain protein monitored by 2D NMR spectroscopy and amide proton exchange experiments, however, showed that the IF domain experiences a reduced local stability under both native and unfolding conditions compared to the FKBP domain. Nevertheless, the entire protein shows highly cooperative unfolding at elevated denaturing conditions. This cooperativity is significantly reduced in a SlyD<sup>\*</sup> variant missing the IF domain. The quite low local stability due to high internal fluctuations of the IF domain might be the prerequisite for the ubiquitous chaperone function of SlyD. One physiological role of the metallochaperone SlyD is divalent cations binding. Nickel binds only to the FKBP domain but extensively increases the thermodynamic stability of both SlyD domains, verifying the coupled stability of the domains.



SlyD (*sensitive to lysis D*)<sup>1</sup> belongs to the FK506 binding protein (FKBP) family and exhibits peptidylprolyl isomerase and chaperone properties leading to a very efficient protein folding helper enzyme.<sup>2</sup> It was originally discovered in *Escherichia coli* as a host factor for the bacteriophage  $\Phi$ X174 lysis cycle<sup>1</sup> but was also known as a persistent contaminant of recombinantly produced proteins that were purified by nickel ion affinity chromatography.<sup>3,4</sup> SlyD from *E. coli* (*EcSlyD*) contains 196 residues and shares 28.1% sequence identity with human FKBP12 (*hFKBP12*), the prototype of the FKBP family. SlyD homologues are widely distributed among different organisms. All of them have in common a two-domain structure with an FKBP domain and an internal extension of 45–65 residues which are inserted in the flap region (IF domain, *insert in flap*)<sup>5</sup> (Figure S1). Recently, the solution NMR structure of the variant 1–165 of *EcSlyD* which lacks the unstructured C-terminus termed SlyD<sup>\*</sup><sup>6</sup> and the crystal structure of the full length thermophilic homologue *TtSlyD*<sup>7</sup> were solved. Both confirm the typical FKBP secondary structure elements of a four-handed  $\beta$ -sheet ( $\beta 2$ – $\beta 5$ ) and between  $\beta 5$  and  $\beta 2$  an  $\alpha$ -helix ( $\alpha 1$ ) (Figure 1A). Compared to *hFKBP12* and the archaeal *MtFKBP17*, a SlyD-like, structurally and functionally related PPIase from *Methanococcus thermolithotrophicus*,<sup>5</sup> SlyD proteins comprise an additional  $\alpha$ -helix ( $\alpha 4$ ) at the C-terminus. In the crystal structure this additional  $\alpha$ -helix reveals a nickel ion binding motif. The IF domain consists of four short  $\beta$ -strands ( $\beta 6$ – $\beta 9$ ) and one short  $\alpha$ -helix ( $\alpha 3$ ). The

surface of this domain is mainly determined by hydrophobic and negatively charged residues accounting for its excellent chaperone properties. Although both domains are well resolved in the NMR structure of SlyD<sup>\*</sup>, a fixed relative orientation to each other is missing. *TtSlyD* crystallized into three different crystal forms, each of them exhibiting a defined structure with different orientations of the IF domain. This indicates high flexibility of the two domains relative to each other, which might be crucial for a very efficient protein folding helper property. This was also observed in the very recently published solution NMR structure of full-length *EcSlyD* and by NMR relaxation experiments.<sup>7,8</sup>

Mutational analyses showed that the PPIase function is hosted in the FKBP domain and the chaperone activity in the IF domain.<sup>2,9</sup> Substrate binding studies with SlyD<sup>\*</sup> monitored by NMR spectroscopy confirmed this domain separation of activities<sup>6</sup> (see also Kovermann, M., unpublished data). FkpA,<sup>10,11</sup> SurA,<sup>12</sup> and trigger factor<sup>13,14</sup> are also prolyl isomerases with chaperone properties hosted by separate domains. The functional separation of domains goes along with an effective interplay between them to enhance the overall PPIase activity as shown by NMR relaxation data.<sup>15</sup>

**Received:** January 14, 2011

**Revised:** July 13, 2011

**Published:** July 19, 2011

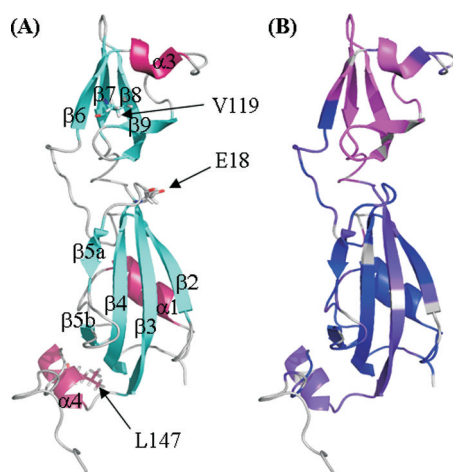


**Figure 1.** Three-dimensional solution NMR structure of SlyD\* (PDB 2K81). (A)  $\beta$ -Sheets are marked in cyan, and  $\alpha$ -helices are shown in dark pink. Secondary structure elements are numbered corresponding to the structure of hFKBP12 (PDB 1FKF). The IF domain is depicted above the FKBP domain. The side chains of three representative amino acids are shown in stick representation. (B) Symbolization of residues during the urea-induced unfolding of SlyD\*. Blue: residues that show a cooperative transition; purple blue: residues that show a steep baseline for the native state and a sharp transition region; magenta: residues that do not show a native baseline and no significant transition region, which mainly comprises residues of the IF domain. Noticeable,  $\beta$ -sheet  $\beta$ 3, returning from the IF domain, differs apparently from the other  $\beta$ -sheets building the core of the FKBP domain. Figures were created using PyMol (DeLano Scientific LLC, 2006).

On the basis of the combination of prolyl isomerase activity, ubiquitous chaperone activity, and metal binding properties, different cellular functions have been proposed for SlyD. Recently, it was shown that SlyD from *E. coli* is involved in the Tat-dependent translocation of folded proteins across membranes.<sup>16</sup> It is assumed that SlyD (as a chaperone) binds to the unstructured Tat-signal sequences and protects them from proteolytic attack in the cytoplasm while they are transported to the membrane. In addition, the participation of SlyD in the biosynthesis of the NiFe hydrogenase 3 in *E. coli*<sup>17–19</sup> and similarly of urease<sup>20,21</sup> was demonstrated. Both enzymes need nickel in their catalytic metal center. Because full length SlyD can bind three to seven nickel ions,<sup>22,23</sup> a function as a nickel transporter is discussed. During the biosynthesis of the NiFe hydrogenase different accessory factors are applied.<sup>24</sup> SlyD directly interacts with the nickel-binding accessory factor HypB via its chaperone domain, inducing a displacement of the bound nickel ions which are then built into the metal center of the hydrogenase precursor form.

The chaperone domain itself can bind a wide range of hydrophobic and positively charged peptides and partially or fully unfolded proteins. Most of proline-limited refolding reactions of substrate proteins are catalyzed by the prolyl isomerase function. Additionally, metal-binding reversibly inhibits the prolyl isomerase function,<sup>22</sup> and the metal binding properties of the metallochaperone SlyD moved very recently again into the focus.<sup>7,23</sup> This ubiquitous function of SlyD requires a high amount of structural flexibility. An appropriate balance between molecular stability and structural flexibility is a prerequisite for the proper function of an enzyme. In order to account for the structure–function relationship of SlyD, we

analyzed the local thermodynamic stability of SlyD\* with several biophysical methods, especially by using NMR spectroscopy. Urea-induced unfolding transitions were monitored by 2D NMR spectroscopy to reveal stability parameters on a residue-by-residue basis. Additionally, native state amide proton exchange experiments show a clear separation of local stability of the two domains in SlyD\*. The residues of the IF domain strongly deviate in terms of local thermodynamic stability from residues of the FKBP domain in the absence of denaturant, providing evidence for its high internal fluctuations, which is essential for its ubiquitous chaperone activity. At elevated denaturant concentrations, complete unfolding of SlyD\* occurs. Therefore, for the global unfolding of SlyD\* a coupling of both domains could be revealed and verified by SlyD\*– $\Delta$ IF.

## MATERIALS AND METHODS

**Materials and Reagents.** Urea ultrapure was purchased from Gerbu (Gaiberg, Germany). All other chemicals were of analytical grade and from Merck (Darmstadt, Germany), Roth (Karlsruhe, Germany), or Sigma-Aldrich (St. Louis, MO).

**Gene Construction, Protein Expression, and Purification.** SlyD\* (*E. coli* SlyD\*(1–165)) was expressed and purified as described elsewhere<sup>25</sup> using a slightly modified procedure where the crude extract with natively folded SlyD\* was applied onto the nickel ion affinity chromatography column and then unfolded and refolded while bound to the column material to wash out tightly bound proteins and peptides. The sequence of SlyD(1–155) derived from the *E. coli* SlyD\*(1–165) gene was inserted into the pETSUMOadapt vector<sup>26</sup> with SUMO as the N-terminal fusion tag arranged with an N-terminal hexahistidine tag for purification via nickel ion affinity chromatography. After cleavage of SUMO with the highly specific SUMO protease Ulp1<sup>27</sup> a second nickel ion affinity chromatography yielded SlyD(1–155), which was further purified by size exclusion chromatography. <sup>15</sup>N-labeling was performed using M9 minimal medium containing 1 g/L <sup>15</sup>N-NH<sub>4</sub>Cl for expression; unlabeled protein was expressed in dYT medium.

**Spectroscopic Measurements.** All spectroscopic measurements were performed in 50 mM sodium phosphate (pH 7.5) and 100 mM sodium chloride at 15 °C. Fluorescence spectra were recorded at a JASCO FP-6500 fluorescence spectrometer. Protein concentrations were determined by absorbance at 280 nm at a JASCO V-660 absorbance spectrometer, using the following extinction coefficients: 5788 M<sup>-1</sup> cm<sup>-1</sup> (SlyD\*, SlyD155), 4470 M<sup>-1</sup> cm<sup>-1</sup> (SlyD\*– $\Delta$ IF), and 2980 M<sup>-1</sup> cm<sup>-1</sup> (IF domain). The concentration of urea was determined by refraction of the solution.<sup>28</sup>

**NMR Measurements.** All NMR spectra were acquired in 50 mM sodium phosphate (pH 7.5), 100 mM sodium chloride, containing 10% (v/v) D<sub>2</sub>O, at 15 °C on a Bruker Avance III 600 (proton resonance frequency 600 MHz). The spectra were processed using NMRPipe<sup>29</sup> and analyzed using NMRView.<sup>30</sup>

**Folding Experiments.** Equilibrium urea-induced unfolding transitions were monitored either by fluorescence spectroscopy or by NMR spectroscopy. For each data point one spectrum was measured. Fluorescence spectra were recorded from 300 to 400 nm after excitation at 280 nm. The NMR monitored unfolding transitions were performed using two NMR tubes: one contained natively folded protein and the other one unfolded protein in 6 M urea. After exchanging a certain volume of protein solution of each tube 2D <sup>1</sup>H/<sup>15</sup>N-

**Table 1. Thermodynamic Parameters Derived from Urea-Induced Unfolding Transitions of SlyD\* and SlyD\*-ΔIF<sup>a</sup>**

	SlyD*			SlyD*-ΔIF		
	fluorescence	TROSY spectra <sup>b</sup>	fluorescence (Zoldák) <sup>c</sup>	fluorescence	TROSY spectra <sup>d</sup>	fluorescence (Zoldák) <sup>c</sup>
$\Delta G_U(\text{H}_2\text{O})$ , kJ/mol	$18.4 \pm 0.6$	$17.7 \pm 3.7$	14.2	$13.9 \pm 0.5$	$13.6 \pm 1.4$	12
$m$ , kJ/(mol M)	$6.9 \pm 0.2$	$8.0 \pm 1.4$	6.4	$3.2 \pm 0.1$	$4.7 \pm 0.6$	4.6
$[D]_{1/2}$ , M	2.7	2.2	2.2	4.3	2.9	2.6

<sup>a</sup>Unfolding transition curves were measured at 15 °C in 50 mM Na<sub>2</sub>HPO<sub>4</sub>, 100 mM NaCl, pH 7.5. Listed errors result from the nonlinear least-squares fit to an apparent two-state model. <sup>b</sup>The depicted stability value is the mean value of the stabilities of all residues from the FKBP domain that could be fitted by an apparent two-state model (residues colored blue in Figure 1B). <sup>c</sup>Stability parameters were taken from ref 38. These transition curves were measured at 25 °C in 100 mM KH<sub>2</sub>PO<sub>4</sub>, pH 7.5. <sup>d</sup>The depicted stability value is the mean value of the stabilities of all residues that could be fitted by an apparent two-state model.

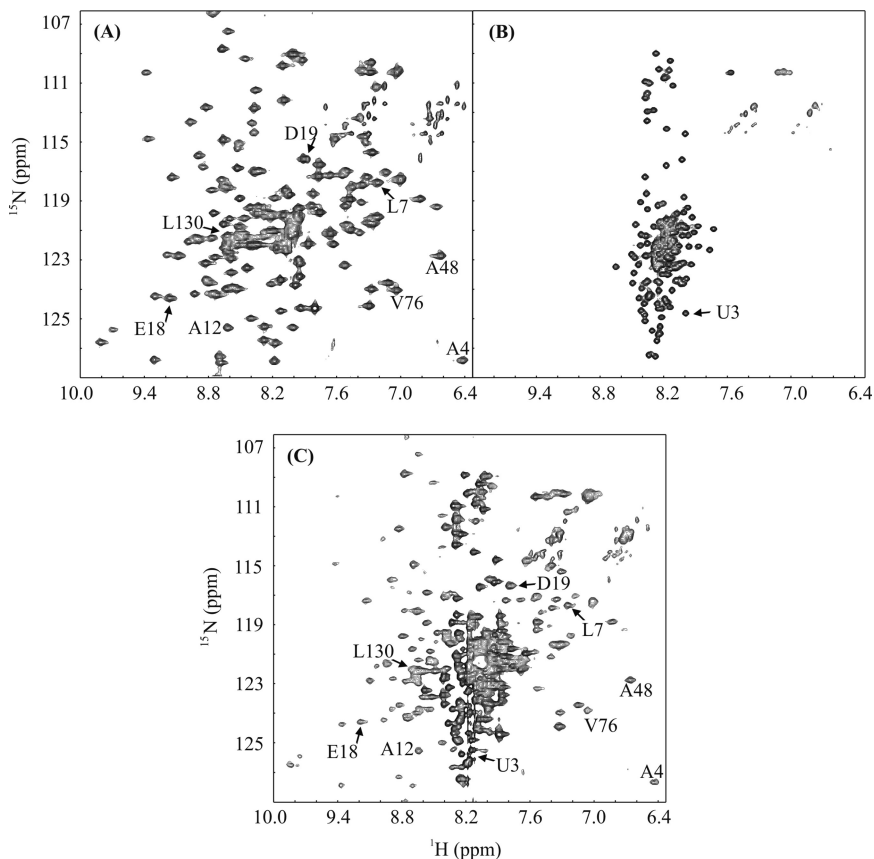
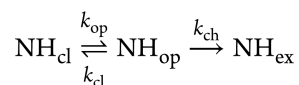


**Figure 2.** <sup>1</sup>H/<sup>15</sup>N-TROSY-HSQC spectra recorded during the urea-induced unfolding of SlyD\*. (A) Spectrum of SlyD\* in the absence of urea, (B) in the presence of 5.5 M urea for the unfolded state, and (C) in the presence of 2.2 M urea at the transition midpoint. Unfolding was measured at 15 °C in 50 mM sodium phosphate (pH 7.5) and 100 mM sodium chloride with a protein concentration of 0.67 mM. For some amide protons which could be analyzed by an apparent two-state model the assignment is indicated in the spectra and respective transition curves are shown in Figure 3.

TROSY-HSQC spectra were recorded after equilibrium has reached. Data were analyzed according to an apparent two-state model by nonlinear least-squares fit to obtain the Gibbs free energy of unfolding  $\Delta G_U(\text{H}_2\text{O})$  as a function of urea using GraFit 5.

**Amide Proton Exchange Experiments.** H/D exchange reactions were started by a fast buffer exchange of protonated <sup>15</sup>N SlyD\* (or <sup>15</sup>N SlyD\*-ΔIF) into 100% D<sub>2</sub>O, containing 50 mM sodium phosphate (pD 7.5) and 100 mM sodium chloride at 15 °C. After a dead time of 7 min, a series of 110 2D <sup>1</sup>H/<sup>15</sup>N-TROSY-HSQC spectra were recorded during an exchange time of 73 h. For some fast exchanging amide protons an additional H/D exchange experiment was performed recording spectra in intervals of 5 min. Further H/D exchange

experiments of <sup>15</sup>N SlyD\* were performed in the presence of 0.62, 1.07, and 1.66 M urea to implement the native-state hydrogen exchange theory.<sup>31–34</sup> Each amide proton can exist in two conformations: the open and therefore exchange-competent state (NH<sub>op</sub>) and the closed state (NH<sub>cl</sub>). The opening and closing rates of protected H-bonds are defined by  $k_{op}$  and  $k_{cl}$ . The observed exchange rate with solvent molecules is then described as  $k_{ex}$ .



The H/D exchange provides amide exchange rate constants  $k_{ex}$  for each amide proton which were determined by fitting a single-exponential function to the volume decay of the amide

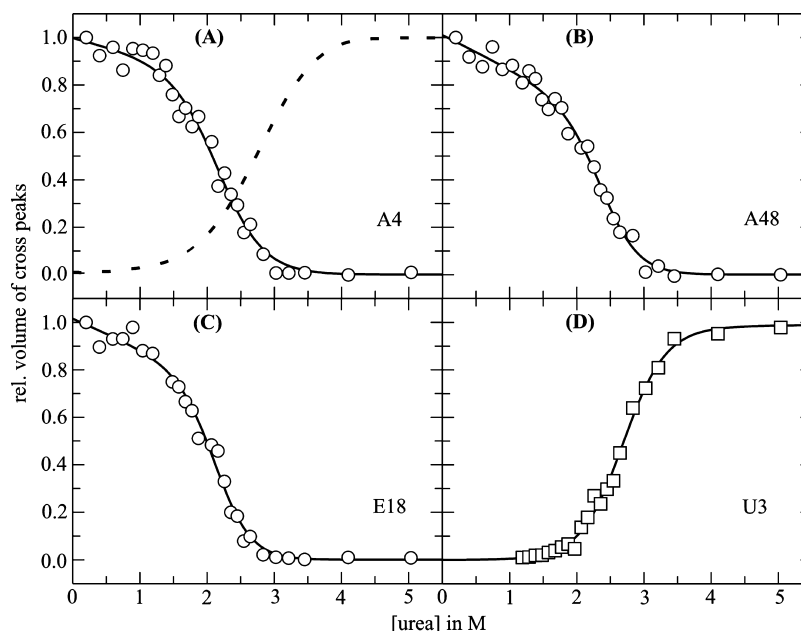


**Figure 3.** Urea-induced unfolding transition curves for selected residues of SlyD\* (Ala 4 (A), Ala 48 (B), Glu 18 (C), unfolded residue Unf 3 (D)), monitored by a series of 2D  $^1\text{H}/^{15}\text{N}$ -TROSY-HSQC spectra at 15 °C in 50 mM sodium phosphate (pH 7.5) and 100 mM sodium chloride, 10%  $\text{D}_2\text{O}$  (v/v). Solid lines represent a fit of an apparent two-state model (results are given in Table 1). (A) A direct comparison for transition curves of the folded (open circles, A4) and unfolded (dashed line, U3) state is depicted.

proton cross-peaks. With the help of  $k_{\text{ex}}$ , protection factors  $P$  were determined according to  $P = k_{\text{ch}}/k_{\text{ex}}$  with  $k_{\text{ch}}$ , the intrinsic exchange rate constant derived from peptide models.<sup>35</sup> For well-protected amide protons, the validity of the EX2 regime was confirmed by additional exchange experiments at pH 6.0 and 9.0 (data not shown).

Exchange processes in the millisecond time regime were analyzed by fast amide proton exchange monitored by a modified MEXICO technique based on  $^1\text{H}/^{15}\text{N}$ -HSQC spectra.<sup>36,37</sup> The rate constants for proton exchange  $k_{\text{ex}}$  for each amide proton were determined by fitting the volume increase of the amide proton cross-peaks with a double-exponential function according to Hofmann et al.<sup>37</sup>

## RESULTS

**Urea-Induced Unfolding Transitions.** Thermodynamic stability of SlyD\* and SlyD\* $\cdot\Delta\text{IF}$  was determined by urea-induced unfolding transitions monitored by fluorescence spectroscopy providing data related to previous results<sup>9,25</sup> and underlined an unfolding mechanism which follows an apparent two-state model (Table 1). The presence of nickel ions strongly increased the overall stability by 9 kJ/mol to  $27.1 \pm 1.3$  kJ/mol (Figure S2) without changing the cooperativity ( $m = 7.0 \pm 0.3$  kJ/(mol M)). This result was observed for SlyD(1–155), which was truncated according to the sequence alignment with *Tt*SlyD (Figure S1) to only have this single metal binding site found for *Tt*SlyD. SlyD(1–155) shows a comparable stability to SlyD\*.

This apparent two-state scenario of unfolding of SlyD\* monitored by few fluorophores can be analyzed in much more detail by  $^1\text{H}$ – $^{15}\text{N}$  NMR spectroscopy with residue-by-residue resolution along the peptide chain. Urea-induced unfolding transition curves of SlyD\* and SlyD\* $\cdot\Delta\text{IF}$  were detected by 2D  $^1\text{H}/^{15}\text{N}$ -TROSY-HSQC spectra. Signals for the native state showed a volume decrease of the respective cross-peaks and

disappeared whereas signals for the unfolded state appeared at a different chemical shift showing an increasing cross-peak volume (Figure 2). If the protein follows a two-state mechanism of denaturant-induced unfolding at equilibrium, the NMR intensities of all residues should follow the same transition because they correspond to either the native or the unfolded population. Such a scenario has been observed for several proteins including Orf56<sup>39</sup> and barstar.<sup>37</sup> SlyD\* deviates from such a simple two-state mechanism, when comparing the NMR detected transition curves of individual residues. To identify residues, which follow and which deviate from two-state behavior, we analyzed all transition curves assuming an apparent two-state model, bearing in mind that folding of the entire ensemble is much more complex. Following this approach, deviations from two state manifest in very steep apparent native baselines. These residues experience indeed a conformational transition at low urea concentrations, and therefore, this apparent native baseline should not be mistaken as the real native baseline, which we cannot determine experimentally for these residues.

One set of residues (Figure 3) provided values for the Gibbs free energy of around  $17.7 \pm 3.7$  kJ/mol by this approach, which was in agreement with those measured by fluorescence spectroscopy (Table 1), and therefore we assume for these residues a cooperative unfolding transition and colored them blue in Figure 1B. The majority of residues from the FKBP domain (from Asp 3 to Ser 64) belongs to this set. A direct comparison of transition curves for the folded and unfolded state (Figure 3A), however, shows different transition midpoints, and their cross-point strongly deviates from 0.5 (relative cross-peak volume), which shows already the limitations of this approach. We did not observe an intermediate species because no additional cross-peaks in the 2D spectra could be detected (Figure 2A–C). Partially folded intermediates and additional cross-peaks were indeed observed

e.g. during unfolding of p19<sup>INK4d40</sup> or tANK,<sup>41</sup> which is not the case for the here presented SlyD\*.

A second set of resonances within the FKBP domain, especially residues from  $\beta$ -sheet  $\beta_3$ , which follows the linking residues from the IF domain, and from  $\alpha$ -helix  $\alpha_4$  exhibited transition curves with steep apparent baselines for the native state (purple in Figures 1B and 4). A third set of resonances

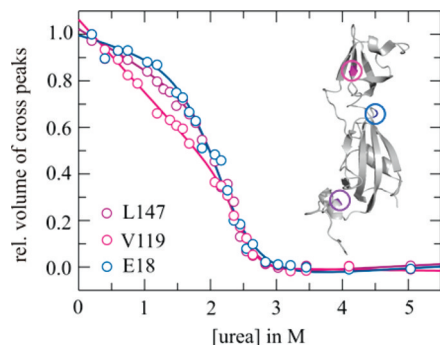


**Figure 4.** Three representative urea-induced unfolding transition curves. Curves for selected residues of SlyD\* indicated at the structure were monitored by 2D  $^1\text{H}/^{15}\text{N}$ -TROSY-HSQC spectra at 15 °C in 50 mM sodium phosphate (pH 7.5), 100 mM sodium chloride, 10%  $\text{D}_2\text{O}$  (v/v). The representative residues are also depicted in stick representation in Figure 1A.

comprises about half of the residues from the IF domain, which show a very steep linear signal intensity decrease of the cross-peaks between 0 and 1.5 M urea (magenta in Figures 1B and 4).

Surprisingly, significant differences in curve progression of these three sets of residues are only apparent between 0 and 2 M urea where the native state population dominates. After the transition midpoint at higher urea concentrations the transition curves coincide (Figure 4). Note that the fluorescence detected urea transition is not sensitive to these events between 0 and 2 M urea, where we find a straight native baseline (see e.g. open circles in Figure S2).

Urea-induced unfolding transitions monitored by 2D  $^1\text{H}/^{15}\text{N}$ -TROSY-HSQC spectra were also performed with SlyD\*- $\Delta\text{IF}$ , which lacks the IF domain and thus represents the unfolding properties of the isolated FKBP domain. The majority of the residues followed coinciding unfolding behavior with a mean value of  $13.6 \pm 1.4$  kJ/mol for the Gibbs free energy and  $4.7 \pm 0.6$  kJ/(mol M) for the  $m$  value, supporting data from fluorescence measurements (Figure 5B, Table 1). All of these residues showed well-defined, horizontal baselines for the native state including the residues from  $\beta$ -sheet  $\beta_3$  and  $\alpha$ -helix  $\alpha_4$  (Figure 5A). Compared to SlyD\*, the extrapolated Gibbs free energy at 0 M urea and the cooperativity of the isolated FKBP domain are reduced. The reduction of both values causes the surprising observation that at about 3 M urea all SlyD\* molecules are unfolded, whereas only about half of the SlyD\*- $\Delta\text{IF}$  molecules have unfolded.

An analogous experiment for the isolated IF domain could not be carried out because of its highly reduced stability under these conditions. However, the 2D  $^1\text{H}/^{15}\text{N}$ -HSQC spectrum recorded in the presence of stabilizing 0.5 M ammonium sulfate displayed two peak populations representing the native and unfolded states with nearly 30% relative signal intensity for the

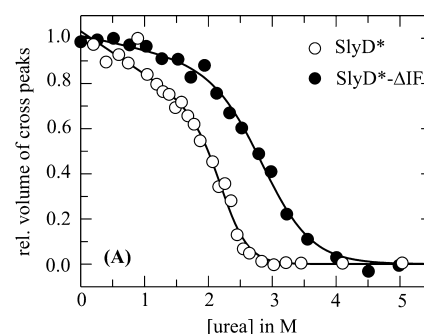


**Figure 5.** Comparison of NMR-detected urea-induced unfolding transition of SlyD\* (open circles) and SlyD\*- $\Delta\text{IF}$  (closed circles) of Leu 147 measured at 15 °C in 50 mM sodium phosphate (pH 7.5) and 100 mM sodium chloride, 10%  $\text{D}_2\text{O}$  (v/v). Continuous lines represent a fit of a two-state model to both transitions.

native state (Figure S3). It is noteworthy that these 30% were active in a standard chaperone assay (data not shown).

**Amide Proton Exchange Experiments.** NMR-based amide proton exchange experiments were applied to measure the local stability of SlyD\* in the absence of denaturants with residue resolution. First, slow hydrogen/deuterium (H/D) exchange was detected by dissolving protonated SlyD\* in  $\text{D}_2\text{O}$  to follow high local protection. These residues are predominantly located in the FKBP domain (Figure 6B). Most of the residues of the IF domain exchanged within the experimental dead time of 7 min and could not be analyzed. Provided that they were detected, residues of the IF domain showed 1000-fold reduced protection factors compared to the well-protected residues from the FKBP domain. Very high protection was detected for the central  $\beta$ -sheets of the FKBP domain ( $\beta_2$ – $\beta_4$ ) (Figure 6A). As expected, loop regions hardly showed any protection. Exchange processes in a time regime of 10–500 ms corresponding to very low protected amides were accessible with the modified MEXICO technique (Figure S5).<sup>36</sup> Some more residues of the IF domain as well as residues from loop regions in the FKBP domain could be analyzed by this NMR technique. The heterogeneity in the protection factors of SlyD\* between IF domain and FKBP domain (Figure 6) indicates a diversity in the local stability of the two domains.

**Native State Hydrogen Exchange Theory.** In order to get a more detailed view on possible folding subunits, the native state hydrogen exchange theory was applied, which combines both approaches, H/D exchange and urea-induced unfolding. H/D exchange experiments in the presence of increasing denaturant concentrations still enclosing the native state can reveal folding subunits.<sup>32–34</sup> The calculated free energy of stabilization  $\Delta G_{\text{HD}}$  for each denaturant concentration plotted against the denaturant concentration shows then a different curve progression and different slope ( $m$  value) for residues from different folding subunits. These  $m$  values plotted against the stabilization energy at 0 M denaturant for each residue should manifest an arrangement in groups of residues corresponding to the same folding subunit.

For SlyD\*, H/D exchange experiments were performed in the presence of three different urea concentrations. Only amide protons well protected in the absence of urea were considered and therefore only residues from the FKBP domain. As expected, stability was decreased upon increasing urea concentrations (Figure S6A). All analyzable residues showed

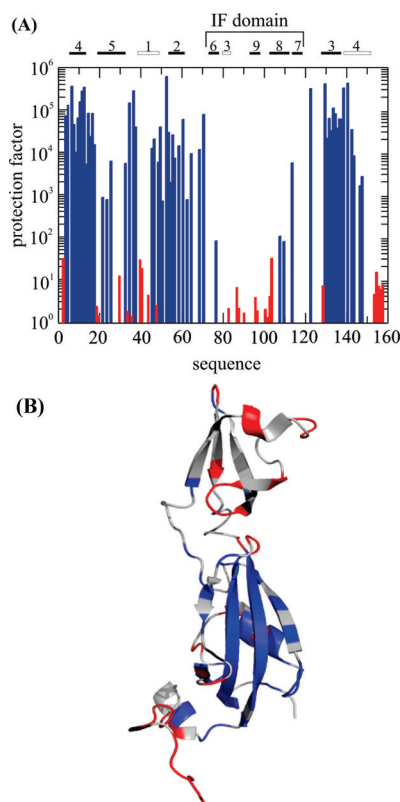


**Figure 6.** Local stability of SlyD\* determined by amide proton exchange experiments at 15 °C in 50 mM sodium phosphate (pH 7.5) and 100 mM sodium chloride. (A) Protection factors of backbone amides of SlyD\* detected by H/D exchange (blue bars) and fast amide proton exchange (MEXICO technique, red bars) are shown in a logarithmic scale. Missing bars indicate either residues that were not accessible by both exchange experiments or not assigned residues. The position of the IF domain is indicated at the top. Rectangles symbolize secondary structure elements (filled rectangles:  $\beta$ -sheets; open rectangles:  $\alpha$ -helices). (B) Residues with highly protected amide protons against solvent exchange measured by H/D exchange ( $P > 10^2$ ) are indicated in blue on the structure of SlyD\*. Hardly protected backbone amides detected by fast amide proton exchange with the modified MEXICO experiment ( $P < 10^2$ ) are shown in red. Residues not accessible by either H/D or MEXICO because of very fast amide proton exchange are indicated in gray; amides with missing assignment or prolines are shown in black.

the same trend. The expected difference for residues of strand  $\beta 3$  and helix  $\alpha 4$  compared to other residues from the FKBP domain during the urea-induced unfolding transitions monitored by chemical shift changes in 2D NMR spectra was not found in this analysis. Likewise, no clustering of residues into defined groups, e.g. representing secondary structural elements, was observed, indicating that the FKBP domain of SlyD\* unfolds uniformly in one folding unit and does not exhibit folding subunits (Figure S6B).

## DISCUSSION

Amide proton exchange monitored by NMR allows to study the local stability of proteins. For SlyD\*, we found a strongly reduced stability for the IF domain compared to the FKBP domain, indicating high local fluctuation required for fast exchange. These fluctuations might be advantageous for the chaperon function of SlyD\*, which unspecifically binds to unfolded or partially folded protein substrates.<sup>37</sup> Additionally,

the IF domain also stands out concerning its high dynamics on a nano- to picosecond time scale monitored by <sup>15</sup>N relaxation.<sup>15</sup> This study also revealed that there has to be a cross-talk between the two domains not at a structural but at a dynamic level because substrate binding at the IF domain increased the local dynamics of the active site in the FKBP domain at this time scale.

A coupling of the two domains in terms of thermodynamic stability was also observed by the here presented urea-induced unfolding transitions. It is worth mentioning that the two domains of SlyD\* are not sequentially arranged along the primary sequence, but the IF domain is inserted (Leu 75–Asp 120) and the C-terminal residues complete the FKBP domain comprising  $\beta$ -strand 3 and  $\alpha$ -helix 4. These C-terminal residues sense the reduced stability of the IF domain up to 2 M urea (purple in Figure 1B and L147 in Figure 4) by a steeper baseline compared to most of the other residues of the FKBP domain (blue in Figure 1B). The thermodynamic coupling becomes further evident by the addition of Ni<sup>2+</sup>. Divalent cations bind to SlyD\* at the interface of the C-terminal  $\alpha$ -helix 4 and the FKBP domain.<sup>8,42</sup> Not only residues from the FKBP domain but also from the IF domain show increased stability and a flat baseline in the NMR detected unfolding transitions (see e.g. M94 of the IF domain in Figure S2A). Physiologically, it was shown that SlyD is involved in the biosynthesis of NiFe hydrogenase 3 from *E. coli* by interacting with the accessory factor HypB.<sup>18,43</sup> By complex formation between SlyD and HypB nickel delivery from the nickel binding enzyme HypB is enforced by the metallochaperone SlyD. At a molecular level, the PPIase activity of full length SlyD gets reversibly inhibited by Ni<sup>2+</sup> ions, and this influence disappears after truncation of the C-terminus including  $\alpha$ -helix 4.<sup>22</sup> Thus, Ni<sup>2+</sup> binding modulates both the thermodynamically and functionally tightly coupled properties of the IF and FKBP domain.

The residue resolution of the urea-induced unfolding transitions can be employed to characterize the ensemble properties of SlyD\* at increasing urea concentrations. At the midpoint of the transition, half of the chains are unfolded, and this population increases cooperatively toward higher urea concentrations. The other half of protein chains shows a heterogeneous behavior between 0 M urea and the midpoint concerning the IF and FKBP domain. Because of the low cooperativity of unfolding and the low local stability of the small IF domain, about half of this heterogeneous population has an unfolded IF domain at about 1 M urea. At this urea concentration, the majority of the FKBP domain is folded and a small fraction has lost  $\beta$ -strand 3 and  $\alpha$ -helix 4. Because of the higher cooperativity of the FKBP domain, this heterogeneity reduces above 1 M urea and vanished at the midpoint of the transition at 2.2 M urea. Above 2.2 M urea, the native population cooperatively decays until all chains are unfolded. In summary, the two domains of SlyD\* do not unfold like two independent beads on a string but show a coupled thermodynamic stability possibly because the IF domain is inserted in the primary sequence. At low urea concentrations, a fraction of the SlyD\* molecules unfold in the IF domain,  $\beta$ -strand 3 and  $\alpha$ -helix 4. This fraction depopulates at increasing urea concentrations.

The gene-3-protein from the tip of fd phage has also an inserted second domain (N2), and the C-terminus completes the tertiary structure of the N1 domain. N2 is less stable than N1, but because of its high cooperativity, it completely unfolds

at low urea concentrations within the native baseline of N1. Therefore, equilibrium unfolding of N1 is not affected by N2 and superimposes with the transition of isolated N1.<sup>44</sup> On the other hand, H/D exchange of the native state at 0 M urea shows that the stability of both domains are coupled because both domains show equally high protection factors corresponding to the Gibbs free energy of unfolding derived from the urea transition.<sup>45</sup> In the case of the two domain protein yeast hexokinase isoenzyme ScHXk2, where both domains are formed by discontinuous peptide sequences, the ensemble of chains also shows heterogeneous urea dependence, where a very stable unfolding intermediate populates, where only parts of both domains are still folded.<sup>46</sup>

During the urea induced unfolding transitions monitored by NMR, no additional cross-peaks were observed, which might indicate the population of a homogeneous ensemble of a folding intermediate at equilibrium. Such additional cross-peaks could be observed for example for p19<sup>INK4d</sup> and tANK, which verified a folding scheme of  $U \leftrightarrow I \leftrightarrow N$ .<sup>9,40,41</sup> In both cases, the N-terminal helices showed reduced thermodynamic stabilities and were unfolded in I, whereas the C-terminal helices were already in place. Therefore, we can again exclude for the here studied SlyD\* a mechanism, where the IF domain cooperatively unfolds at low urea concentrations and the FKBP domain remains folded.

The thermodynamic coupling of the IF and FKBP domains has also implications for their functional interplay. The prolyl isomerase activity is significantly enhanced in the presence of the IF domain. The earlier observed loose orientation of both domains relative to each other is consistent with very low protection for amides in the linker region between the two domains. The high degree of local fluctuations is carried forward within the IF domain. High opening and closing rates of secondary structure elements in the IF domain might be the prerequisite for the proper function as a ubiquitous applicable chaperone to bind peptides and proteins of nearly all size and shape.<sup>7</sup> It is already known that SlyD\* can bind a wide range of hydrophobic and positively charged substrates and prevent them from aggregation.<sup>6,48–50</sup> The structural plasticity within the IF domain is a well-known feature for chaperones to promote promiscuous substrate binding although this leads to a reduced thermodynamic stability. Various chaperones overcome this problem by different approaches. HdeA, a chaperone that prevents acid-induced protein aggregation, also shows a disordered, partially unfolded substrate binding site which is hidden in the dimeric state at the dimer interface and therefore stabilized.<sup>51</sup> Monomeric, functional HdeA is only present at low pHs. On the other hand, the conformational variability is achieved by intrinsically disordered protrusion segments that are formed upon oligomerization as seen for group II chaperonins.<sup>52</sup>

## ■ ASSOCIATED CONTENT

### ● Supporting Information

Sequence alignment of several bacterial SlyD proteins (Figure S1); <sup>1</sup>H/<sup>15</sup>N-HSQC spectrum for the isolated IF domain (Figure S2); urea-induced unfolding transition curves of SlyD155 in the absence and presence of nickel and the respective stability parameters (Figure S3); kinetic traces of the slow H/D exchange as well as kinetic traces from fast amide proton exchange events monitored by the modified MEXICO technique (Figures S4 and S5); plot of urea-dependent stability

data to underline that no clustering into folding subunits takes place according to the native state hydrogen exchange theory (Figure S6). This material is available free of charge via the Internet at <http://pubs.acs.org>.

## ■ AUTHOR INFORMATION

### Corresponding Author

\*Phone: +49 345 55 28550; Fax: +49 345 55 27161; e-mail: [jochen.balbach@physik.uni-halle.de](mailto:jochen.balbach@physik.uni-halle.de).

### Present Address

<sup>§</sup>Biophysical Chemistry, Lund University, SE-22100 Lund, Sweden.

### Funding

This work was supported by grants of the GRK 1026 and the SFB 610 of the DFG and the Excellence Initiative of the State of Sachsen-Anhalt. Significant investments into our NMR infrastructure from the European Regional Development Fund (ERDF) by the European Union are also gratefully acknowledged.

## ■ ACKNOWLEDGMENTS

Expression vectors for SlyD\* and SlyD\*-ΔIF were kindly provided by Christian Scholz, Roche Diagnostics, Penzberg, Germany. We thank Christian Löw for helpful discussions.

## ■ ABBREVIATIONS

SlyD\*, SlyD (*sensitive to lysis*) from *Escherichia coli* comprising residues from 1 to 165; SlyD\*ΔIF, variant of SlyD\* with the IF domain replaced by the shorter flap of human FKBP12; FKBP, FK506 binding protein; IF, insert in flap; PPIase, peptidylprolyl *cis/trans* isomerase; H/D, hydrogen/deuterium; SUMO, small ubiquitin-like modifier; dYT, double yeast trypton; 1D/2D, 1-/2-dimensional; HSQC, heteronuclear single quantum coherence; TROSY, transverse relaxation optimized spectroscopy; MEXICO, measurement of fast proton exchange rates in isotopically labeled compounds.

## ■ REFERENCES

- (1) Roof, W. D., Horne, S. M., Young, K. D., and Young, R. (1994) slyD, a host gene required for phi X174 lysis, is related to the FK506-binding protein family of peptidyl-prolyl *cis-trans*-isomerases. *J. Biol. Chem.* 269, 2902–2910.
- (2) Scholz, C., Eckert, B., Hagn, F., Schaarschmidt, P., Balbach, J., and Schmid, F. X. (2006) SlyD proteins from different species exhibit high prolyl isomerase and chaperone activities. *Biochemistry* 45, 20–33.
- (3) Arnold, F. H. (1991) Metal-affinity separations: a new dimension in protein processing. *Biotechnology* 9, 151–156.
- (4) Lindner, P., Guth, B., Wülfing, C., Krebber, C., Steipe, B., Müller, F., and Plückthun, A. (1992) Purification of native proteins from the cytoplasm and periplasm of *Escherichia coli* using IMAC and histidine tails: A comparison of proteins and protocols. *Methods* 4, 41–56.
- (5) Suzuki, R., Nagata, K., Yumoto, F., Kawakami, M., Nemoto, N., Furutani, M., Adachi, K., Maruyama, T., and Tanokura, M. (2003) Three-dimensional solution structure of an archaeal FKBP with a dual function of peptidyl prolyl *cis-trans* isomerase and chaperone-like activities. *J. Mol. Biol.* 328, 1149–1160.
- (6) Weininger, U., Haupt, C., Schweimer, K., Graubner, W., Kovermann, M., Brüser, T., Scholz, C., Schaarschmidt, P., Zoldak, G., Schmid, F. X., and Balbach, J. (2009) NMR solution structure of SlyD from *Escherichia coli*: spatial separation of prolyl isomerase and chaperone function. *J. Mol. Biol.* 387, 295–305.
- (7) Kahra, D., Kovermann, M., Löw, C., Hirschfeld, V., Haupt, C., Balbach, J., and Hübner, C. G. (2011) Conformational Plasticity and

Dynamics in the Generic Protein Folding Catalyst SlyD Unraveled by Single-Molecule FRET. *J. Mol. Biol.*, DOI: 10.1016/j.jmb.2011.05.002.

- (8) Martino, L., He, Y., Hands-Taylor, K. L., Valentine, E. R., Kelly, G., Giancola, C., and Conte, M. R. (2009) The interaction of the Escherichia coli protein SlyD with nickel ions illuminates the mechanism of regulation of its peptidyl-prolyl isomerase activity. *FEBS J.* 276, 4529–4544.
- (9) Knappe, T. A., Eckert, B., Schaarschmidt, P., Scholz, C., and Schmid, F. X. (2007) Insertion of a chaperone domain converts FKBP12 into a powerful catalyst of protein folding. *J. Mol. Biol.* 368, 1458–1468.
- (10) Ramm, K., and Plückthun, A. (2000) The periplasmic Escherichia coli peptidylprolyl cis,trans-isomerase FkpA. II. Isomerase-independent chaperone activity in vitro. *J. Biol. Chem.* 275, 17106–17113.
- (11) Saul, F. A., Arie, J. P., Vulliez-le Normand, B., Kahn, R., Betton, J. M., and Bentley, G. A. (2004) Structural and functional studies of FkpA from Escherichia coli, a cis/trans peptidyl-prolyl isomerase with chaperone activity. *J. Mol. Biol.* 335, 595–608.
- (12) Webb, H. M., Ruddock, L. W., Marchant, R. J., Jonas, K., and Klappa, P. (2001) Interaction of the periplasmic peptidylprolyl cis-trans isomerase SurA with model peptides. The N-terminal region of SurA is essential and sufficient for peptide binding. *J. Biol. Chem.* 276, 45622–45627.
- (13) Hesterkamp, T., and Bukau, B. (1996) Identification of the prolyl isomerase domain of Escherichia coli trigger factor. *FEBS Lett.* 385, 67–71.
- (14) Scholz, C., Stoller, G., Zarn, T., Fischer, G., and Schmid, F. X. (1997) Cooperation of enzymatic and chaperone functions of trigger factor in the catalysis of protein folding. *EMBO J.* 16, 54–58.
- (15) Kovermann, M., Zierold, R., Haupt, C., Löw, C., and Balbach, J. (2011) NMR relaxation unravels interdomain crosstalk of the two domain prolyl isomerase and chaperone SlyD. *Biochim. Biophys. Acta* 1814, 873–881.
- (16) Graubner, W., Schierhorn, A., and Brüser, T. (2007) DnaK plays a pivotal role in Tat targeting of CueO and functions beside SlyD as a general Tat signal binding chaperone. *J. Biol. Chem.* 282, 7116–7124.
- (17) Leach, M. R., Sandal, S., Sun, H., and Zamble, D. B. (2005) Metal Binding Activity of the Escherichia coli Hydrogenase Maturation Factor HypB. *Biochemistry* 44, 12229–12238.
- (18) Zhang, J. W., Butland, G., Greenblatt, J. F., Emili, A., and Zamble, D. B. (2005) A role for SlyD in the Escherichia coli hydrogenase biosynthetic pathway. *J. Biol. Chem.* 280, 4360–4366.
- (19) Zhang, J. W., Leach, M. R., and Zamble, D. B. (2007) The peptidyl-prolyl isomerase activity of SlyD is not required for maturation of Escherichia coli hydrogenase. *J. Bacteriol.* 189, 7942–7944.
- (20) Stingl, K., Schauer, K., Ecobichon, C., Labigne, A., Lenormand, P., Rousselle, J.-C., Namane, A., and de Reuse, H. (2008) In vivo interactome of Helicobacter pylori urease revealed by tandem affinity purification. *Mol. Cell Proteomics* 7, 2429–2441.
- (21) Benanti, E. L., and Chivers, P. T. (2009) An intact urease assembly pathway is required to compete with NikR for nickel ions in Helicobacter pylori. *J. Bacteriol.* 191, 2405–2408.
- (22) Hottenrott, S., Schumann, T., Plückthun, A., Fischer, G., and Rahfeld, J. U. (1997) The Escherichia coli SlyD is a metal ion-regulated peptidyl-prolyl cis/trans-isomerase. *J. Biol. Chem.* 272, 15697–15701.
- (23) Kaluarachchi, H., Sutherland, D. E. K., Young, A., Pickering, I. J., Stillman, M. J., and Zamble, D. B. (2009) The Ni(II)-Binding Properties of the Metallochaperone SlyD. *J. Am. Chem. Soc.* 131, 18489–18500.
- (24) Li, Y., and Zamble, D. B. (2009) Nickel homeostasis and Nickel regulation: An overview. *Chem. Rev.* 109, 4617–4943.
- (25) Scholz, C., Schaarschmidt, P., Engel, A. M., Andres, H., Schmitt, U., Faatz, E., Balbach, J., and Schmid, F. X. (2005) Functional solubilization of aggregation-prone HIV envelope proteins by covalent fusion with chaperone modules. *J. Mol. Biol.* 345, 1229–1241.
- (26) Bosse-Doenecke, E., Weininger, U., Gopalswamy, M., Balbach, J., MöllerKnudsen, S., and Rudolph, R. (2008) High yield production of recombinant native and modified peptides exemplified by ligands for G-protein coupled receptors. *Protein Expr. Purif.* 58, 114–121.
- (27) Reverter, D., and Lima, C. D. (2004) A basis for SUMO protease specificity provided by analysis of human Senp2 and a Senp2-SUMO complex. *Structure* 12, 1519–1531.
- (28) Pace, C. N. (1986) Determination and analysis of urea and guanidine hydrochloride denaturation curves. *Methods Enzymol.* 131, 266–280.
- (29) Delaglio, F., Grzesiek, S., Vuister, G. W., Zhu, G., Pfeifer, J., and Bax, A. (1995) NMRPipe: a multidimensional spectral processing system based on UNIX pipes. *J. Biomol. NMR* 6, 277–293.
- (30) Johnson, B. A. (2004) Using NMRView to visualize and analyze the NMR spectra of macromolecules. *Methods Mol. Biol.* 278, 313–352.
- (31) Bai, Y. W., Englander, J. J., Mayne, L., Milne, J. S., and Englander, S. W. (1995) Thermodynamic parameters from hydrogen exchange measurements. *Energ. Biol. Macromol.* 259, 344–356.
- (32) Maity, H., Maity, M., Krishna, M. M., Mayne, L., and Englander, S. W. (2005) Protein folding: the stepwise assembly of foldon units. *Proc. Natl. Acad. Sci. U.S.A.* 102, 4741–4746.
- (33) Mayo, S. L., and Baldwin, R. L. (1993) Guanidinium Chloride Induction of Partial Unfolding in Amide Proton Exchange in RNase-A. *Science* 262, 873–876.
- (34) Englander, S. W. (1998) Native-state HX. *Trends Biochem. Sci.* 23, 379–381.
- (35) Bai, Y. W., Milne, J. S., Mayne, L., and Englander, S. W. (1993) Primary Structure Effects on Peptide Group Hydrogen Exchange. *Proteins: Struct., Funct., Genet.* 17, 75–86.
- (36) Gemmecker, G., Jahnke, W., and Kessler, H. (1993) Measurement of fast proton exchange rates in isotopically labeled compounds. *J. Am. Chem. Soc.* 115, 11620–11621.
- (37) Hofmann, H., Weininger, U., Löw, C., Golbik, R. P., Balbach, J., and Ulbrich-Hofmann, R. (2009) Fast Amide Proton Exchange Reveals Close Relation between Native-State Dynamics and Unfolding Kinetics. *J. Am. Chem. Soc.* 131, 140–146.
- (38) Zoldák, G., Carstensen, L., Scholz, C., and Schmid, F. X. (2009) Consequences of domain insertion on the stability and folding mechanism of a protein. *J. Mol. Biol.* 386, 1138–1152.
- (39) Zeeb, M., Lipps, G., Lilie, H., and Balbach, J. (2004) Folding and association of an extremely stable dimeric protein from Sulfolobus islandicus. *J. Mol. Biol.* 336, 227–240.
- (40) Zeeb, M., Rösner, H., Zeslawski, W., Canet, D., Holak, T. A., and Balbach, J. (2002) Protein folding and stability of human CDK inhibitor p19INK4d. *J. Mol. Biol.* 315, 447–457.
- (41) Löw, C., Weininger, U., Neumann, P., Klepsch, M., Lilie, H., Stubbs, M. T., and Balbach, J. (2008) Structural insights into an equilibrium folding intermediate of an archaeal ankyrin repeat protein. *Proc. Natl. Acad. Sci. U.S.A.* 105, 3779–3784.
- (42) Hofmann, H., Weininger, U., Low, C., Golbik, R. P., Balbach, J., and Ulbrich-Hofmann, R. (2009) Fast amide proton exchange reveals close relation between native-state dynamics and unfolding kinetics. *J. Am. Chem. Soc.* 131, 140–146.
- (43) Leach, M. R., Zhang, J. W., and Zamble, D. B. (2007) The role of complex formation between the Escherichia coli hydrogenase accessory factors HypB and SlyD. *J. Biol. Chem.* 282, 16177–16186.
- (44) Kerwitz, Y., Kuhn, U., Lilie, H., Knoth, A., Scheuermann, T., Friedrich, H., Schwarz, E., and Wahle, E. (2003) Stimulation of poly(A) polymerase through a direct interaction with the nuclear



poly(A) binding protein allosterically regulated by RNA. *EMBO J.* 22, 3705–3714.

(45) Weininger, U., Jakob, R. P., Eckert, B., Schweimer, K., Schmid, F. X., and Balbach, J. (2009) A remote prolyl isomerization controls domain assembly via a hydrogen bonding network. *Proc. Natl. Acad. Sci. U.S.A.* 106, 12335–12340.

(46) Lilie, H., Bar, D., Kettner, K., Weininger, U., Balbach, J., Naumann, M., Müller, E. C., Otto, A., Gast, K., Golbik, R., and Kriegel, T. (2010) Yeast hexokinase isoenzyme SchHxk2: stability of a two-domain protein with discontinuous domains. *Protein Eng. Des. Sel.* 24, 79–87.

(47) Myers, J. K., Pace, C. N., and Scholtz, J. M. (1995) Denaturant  $m$  values and heat capacity changes: Relation to changes in accessible surface areas of protein unfolding. *Protein Sci.* 4, 2138–2148.

(48) Bukau, B., Deuerling, E., Pfund, C., and Craig, E. A. (2000) Getting newly synthesized proteins into shape. *Cell* 101, 119–122.

(49) Walter, S., and Buchner, J. (2002) Molecular chaperones—cellular machines for protein folding. *Angew. Chem., Int. Ed.* 41, 1098–1113.

(50) Han, K. Y., Song, J. A., Ahn, K. Y., Park, J. S., Seo, H. S., and Lee, J. (2007) Solubilization of aggregation-prone heterologous proteins by covalent fusion of stress-responsive Escherichia coli protein, SlyD. *Protein Eng. Des. Sel.* 20, 543–549.

(51) Tapley, T. L., Körner, J. L., Bargea, M. T., Hupfeld, J., Schauerte, J. A., Gafni, A., Jakob, U., and Bardwell, J. C. A. (2009) Structural plasticity of an acid-activated chaperone allows promiscuous substrate binding. *Proc. Natl. Acad. Sci. U.S.A.* 106, 5557–5562.

(52) Heller, M., John, M., Coles, M., Bosch, G., Baumeister, W., and Kessler, H. (2004) NMR Studies on the Substrate-binding Domains of the Thermosome: Structural Plasticity in the Protrusion Region. *J. Mol. Biol.* 336, 717–729.